# A COMPARATIVE STUDY OF NON-MONOTONICITY FOR UNIDIRECTIONAL AND CROSS ROLLING OF NIOBIUM SHEET

# VIKTOR GÁL<sup>1</sup> – MÁTÉ SZŰCS<sup>2</sup> – GÁBOR SZABÓ<sup>3</sup> – GYÖRGY KRÁLLICS<sup>4</sup>

**Abstract:** Under cold forming conditions, a niobium plate with  $50 \times 50 \times 4$  mm size was rolled using two different types of technology. In first one, the size and properties of the plates were changed by a unidirectional successive multi-step procedure. In another one, cross-rolling with the same reduction was used to achieve the changes in size and properties. Following the experiments, 3D finite element process modelling was performed with DE-FORM software in order to determine the deformation history and state of the two processes for the same plate thickness. This factor is directly related to the microstructure of the material and its related change. The performed process modelling was controlled by comparing the measured and calculated rolling forces and torques.

**Keywords:** sheet rolling, finite element modelling, non-monotonic deformation, niobium

#### INTRODUCTION

Cross rolling, by changing the workpiece orientation and changing the deformation path, is a way of tailoring texture development to reduce the anisotropic properties of the workpiece [1]. The sample to the rolling plane is rotated by 90° about the normal direction (ND). The most commonly used sequence of stages for cross rolling are the following: Two step cross rolling (TSCR), also known as pseudo-cross rolling, where direction is changed after achieving 50% of the total reduction (*Figure 1.a*).; Multistep cross rolling (MSCR), also known as true cross rolling, where direction is changed after each pass (*Figure 1.b*); Clock rolling (*Figure 1.c*) may be one more way of achieving cross rolling by continuously changing the rolling direction by 90° about ND and if the rotation is 180° instead of 90°, it is called as reverse rolling. Alteration in the rolling direction or deformation path changes the substructure formed in the previous path of deformation, and hence affects the deformation

<sup>&</sup>lt;sup>1</sup> Institute of Material Science and Technology, University of Miskolc H-3515 Miskolc-Egyetemváros, Hungary metgy@uni-miskolc.hu

Institute of Physical Metallurgy, Metal Forming and Nanotechnology, University of Miskolc H-3515 Miskolc-Egyetemváros, Hungary femszmat@uni-miskolc.hu

<sup>&</sup>lt;sup>3</sup> Institute of Metallurgy, University of Miskolc H-3515 Miskolc-Egyetemváros, Hungary szabogabor@uni-miskolc.hu

Institute of Physical Metallurgy, Metal Forming and Nanotechnology, University of Miskolc H-3515 Miskolc-Egyetemváros, Hungary femkgy@uni-miskolc.hu

texture. Cross rolling leads to rolled product of comparatively uniform mechanical properties in all directions.

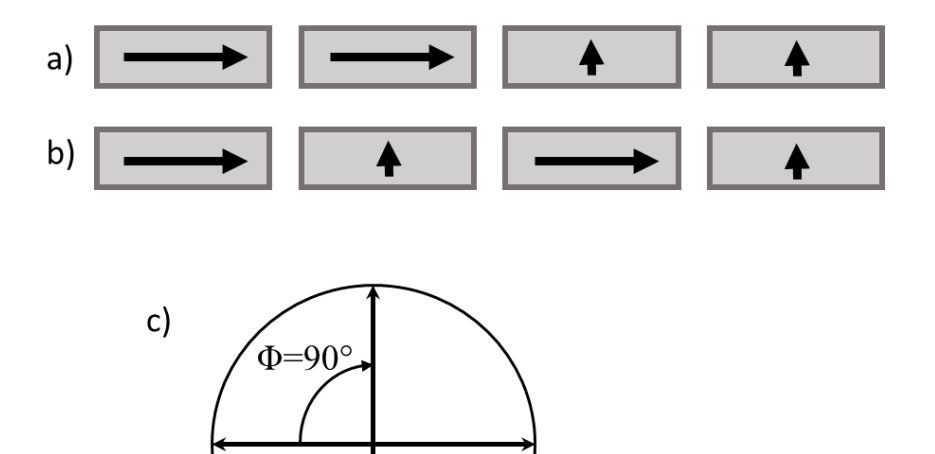


Figure 1
Cross rolling sequences: a) Two-step cross rolling (TSCR)
b) Multistep cross-rolling (MSCR) c) Clock rolling

In present work, the objective of the modelling is to demonstrate the non-monotonic nature of the process, indicating that it is non-monotonic, resulting fine grains and a special crystallographic texture.

# 1. STRAIN HISTORY IN METAL FORMING

The permanent deformation of the samples is demonstrated by the strain trajectory approach as initiated by Ilyushin [2], representing the deviatoric strain tensor (e) in a five-dimensional vector space as:

$$e_{1} = \sqrt{\frac{3}{2}} \ln V'_{11}, \quad e_{2} = \sqrt{2} \left( \ln V'_{22} + \frac{1}{2} \ln V'_{11} \right),$$

$$e_{3} = \sqrt{2} \ln V'_{12}, \quad e_{4} = \sqrt{2} \ln V'_{23}, e_{5} = \sqrt{2} \ln V'_{31}$$
(1)

where  $\ln V$  is the logarithmic deviatoric strain tensor. Some examples for the strain trajectories are shown in *Figure 2*. Trajectory #1 is monotonic, #2 is nearly monotonic, #3 is simple non-monotonic and #4 is cyclic non-monotonic.

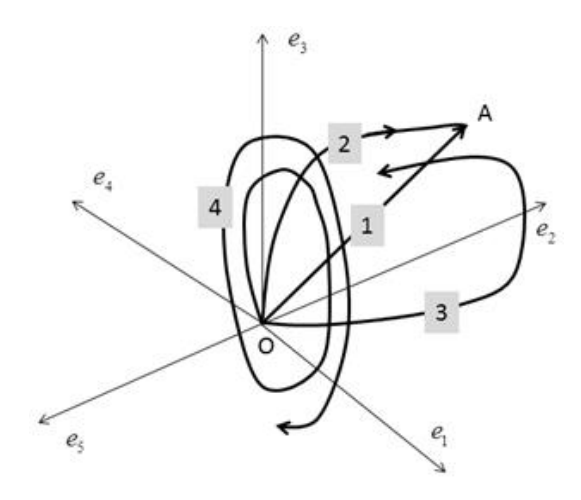


Figure 2

Examples for the strain trajectories in the five-dimensional vector space

In order to appreciate the measure of the non-monotonicity of deformation, consider the nearly monotonic trajectory #2 [3]. During deformation, the endpoint of the strain vector travels along the curved OA trajectory. The ideally monotonic deformation corresponds to the straight-line OA. Therefore, at the deformation time 't' the measure of non-monotonicity is given as:

$$NM(t) = \frac{\overline{\varepsilon}(t)}{\overline{\varphi}(t)} \ge 1 \tag{2}$$

where  $\bar{\varepsilon}(t)$  is the total equivalent strain  $\bar{\varepsilon} = \int_0^t \bar{\varepsilon} dt$ , which is equivalent to the length of the trajectory, and  $\bar{\varphi}(t)$  is the equivalent logarithmic strain, which equals the length of the straight trajectory OA. In the case of non-monotonic deformation, the complete trajectory is separated into n nearly monotonic portions. For each part the  $(NM)_i$  is determined as the ratio of the length of the local trajectory part and the straight segment connecting its end points. In this case, the measure of non-monotonicity of the whole deformation is given as:

$$NM = \sum_{i=1}^{n} (NM)_{i} \tag{3}$$

The larger the value of NM, the higher the degree of non-monotonicity of deformation. It should be noted that although all  $(NM)_i$  values are larger than one, NM may decrease with increasing strain as the end points of the segments may vary during the development of the deformation trajectory.

Strain path change was suggested by Schmitt et al. [4] to measure the change of the direction of the plastic strain tenzor corresponding to the pre strain and to the subsequent strain modes

$$\cos \phi = \frac{\ln \mathbf{V}_{pr} : \ln \mathbf{V}_{sub}}{\left\| \ln \mathbf{V}_{pr} \right\| \left\| \ln \mathbf{V}_{sub} \right\|}$$
(4)

Change in strain path offers an additional parameter during the processing of materials to alter the microstructure and crystallographic texture, and thereby the mechanical properties of the product [5], [6], [7], [8]. In the literature, quite a few articles deal with the finite element simulation of cross rolling [9].

## 2. EXPERIMENTAL ROLLING OF NIOBIUM

The 4 mm thick niobium sheets were unidirectional- and cross rolled at room temperature without any front- and back tension. The other two sizes of material are the same with 50 mm. Both rolling experiments consists of four passes to reach the final thickness of material. The rolls' diameter was 220 mm, and their surfaces were lubricated with a mineral oil-based mixture. The rolling force and torque were recorded in the whole process by an HBM type data acquisition system. *Figure 3* shows the final shapes of sheets which was obtained by the two different technique.

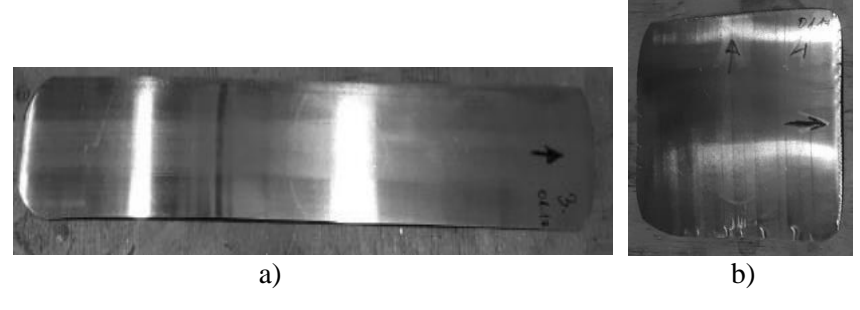


Figure 3
Final shape of rolled niobium after a) the unidirectional- and b) cross rolling

In cross rolling, the material rotated clockwise with angle of  $\Phi = 90^{\circ}$  around its normal axes (perpendicular to sheet plane) before each pass. The entry and final thickness per pass are detailed in *Table 1*. The rolling speed was 30 m/min for each pass.

Table 1

Entry and final thicknesses of unidirectional- and cross rolling per pass

	Unidirectional rolling		Cross rolling		
Pass number	$h_{\theta}$ (mm)	$h_f(mm)$	$h_{\theta}(\mathbf{mm})$	$h_f(mm)$	Ф (°)
1.	4.02	3.46	4.02	3.47	_
2.	3.46	2.98	3.47	3.00	+90°
3.	2.98	2.51	3.00	2.55	-90°
4.	2.51	2.02	2.55	2.11	+90°

#### 3. FINITE ELEMENT ANALYSIS OF NIOBIUM ROLLING

The three-dimensional problem was solved by DEFORM software to simulate the unidirectional- and cross rolling process as well. The rolled material was assumed to be plastic, which flow curves was described by the *Equation* (5).

$$\sigma_{v} = (A + B\overline{\varepsilon}^{n})(1 + C \ln \dot{\varepsilon}^{*}), \quad \dot{\varepsilon}^{*} = \overline{\dot{\varepsilon}} / \overline{\dot{\varepsilon}}_{ref}$$
 (5)

where the material constants are A = 140 MPa, B = 214 MPa, n = 0.525, C = 0.1061, while the roll was rigid. The perfect cylindrical surface of the roll was approximated by 8,000 polynomials. Due to the symmetry of the problem, it was used a half-thick model with a symmetry plane in the middle. In order to achieve the appropriate number of elements in the thickness direction, 8-node brick type mesh elements with a size of  $0.48 \times 0.44 \times 0.71$  mm were used. The total number of elements was 31,000. After the last simulated pass, a minimal distortion of hexahedral mesh was observed, so we used the initial mesh for whole process. The simulation was performed with a constant time step, calculated with the conjugate gradient solver algorithm with direct iteration.

A cold rolling problem was calculated, with an initial plate temperature of 20 °C, and it was assumed that the property of the material did not change during the rolling because of the temperature change. Between each pass, the material was to cool back to ambient temperature of 20 °C. A m = 0.4 Kudo-type friction factor between the plate and cylinder surfaces was used. In the validation process of finite element simulation, the friction factor was modified to minimize the difference between the measured- and calculated force. In *Figure 4* and 5, the diagrams show the measured and calculated rolling force as a function of time.

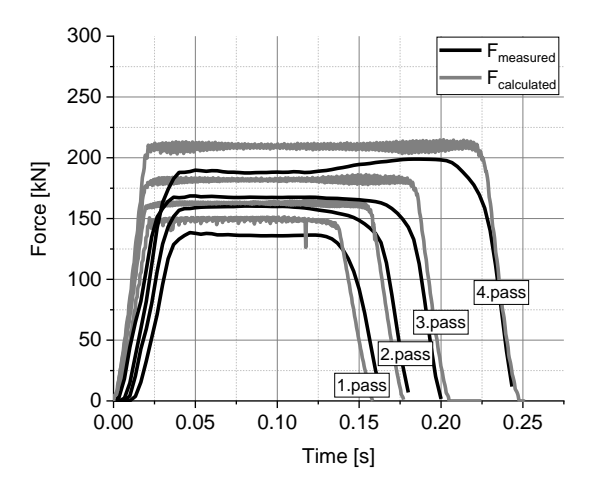


Figure 4

Measured- and calculated force of unidirectional rolling

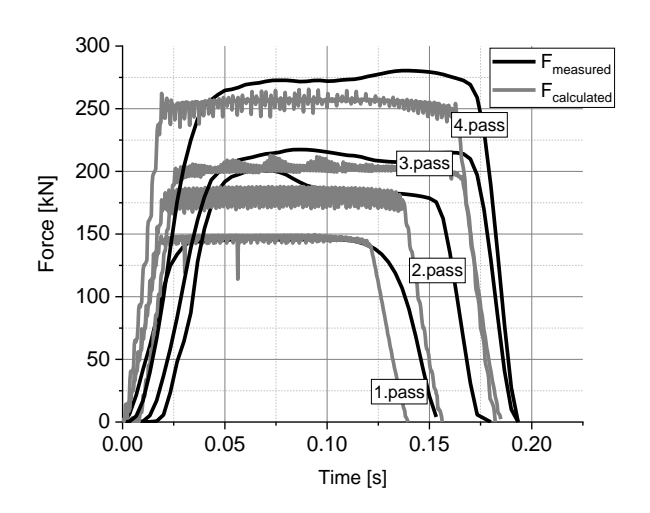


Figure 5
Measured- and calculated force of cross rolling

After the running the simulation, the strain quantities were obtained in six different points through the half thickness of the material. Three of them were selected on the plane of longitudinal section (they are point A, B and C in *Figure 6*) and the other three at the edge of sheet in the same relative coordinates. The relative coordinates of the analysed points along the z axis are the followings,  $r_A = 0.0$   $r_B = 0.5$ ,  $r_C = 1.0$ ,  $r_D = 0.0$   $r_E = 0.5$  and  $r_F = 1.0$ . Each of them are related to the initial position of sheet as it is illustrated by *Figure 6*.

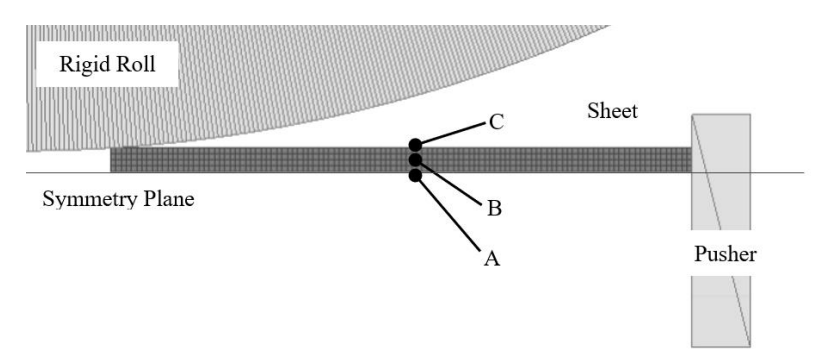


Figure 6
Longitudinal section of 3D finite element model with the position of points A, B and C

## 4. CALCULATION RESULTS OF FINITE ELEMENT ANALYSIS

Below mentioned figures show the analysed quantities in terms of forming time for the unidirectional- and cross rolling as well. The diagrams contain the logarithmic equivalent-  $\bar{\varphi}$ , the total equivalent plastic strain  $\bar{\varepsilon}$  and the parameter of non-monotonicity NM for the whole experimental rolling. The calculation results were obtained in six different material points shown by *Figures 7–12*.

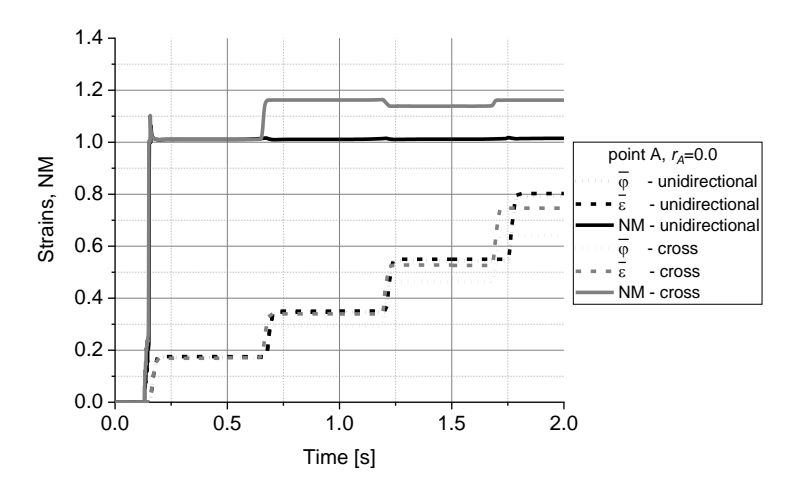


Figure 7

Logarithmic equivalent-, total equivalent strain and NM parameter in terms of time for point A

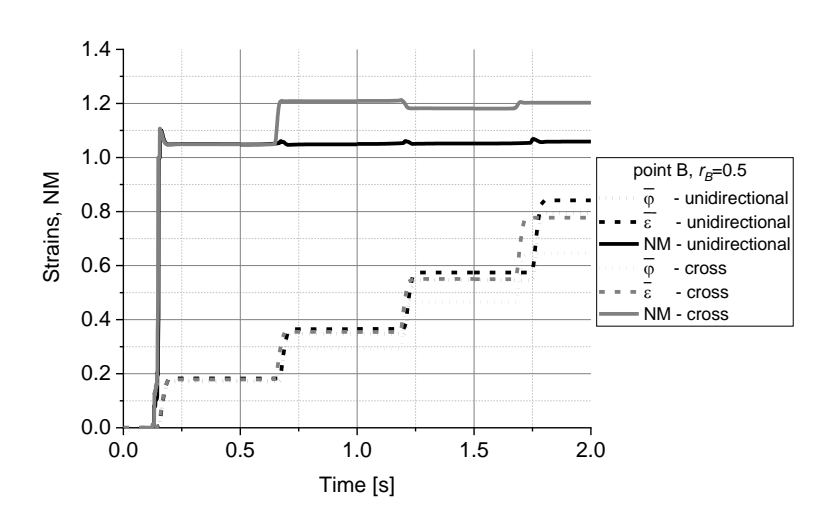


Figure 8

Logarithmic equivalent-, total equivalent strain and NM parameter in terms of time for point B

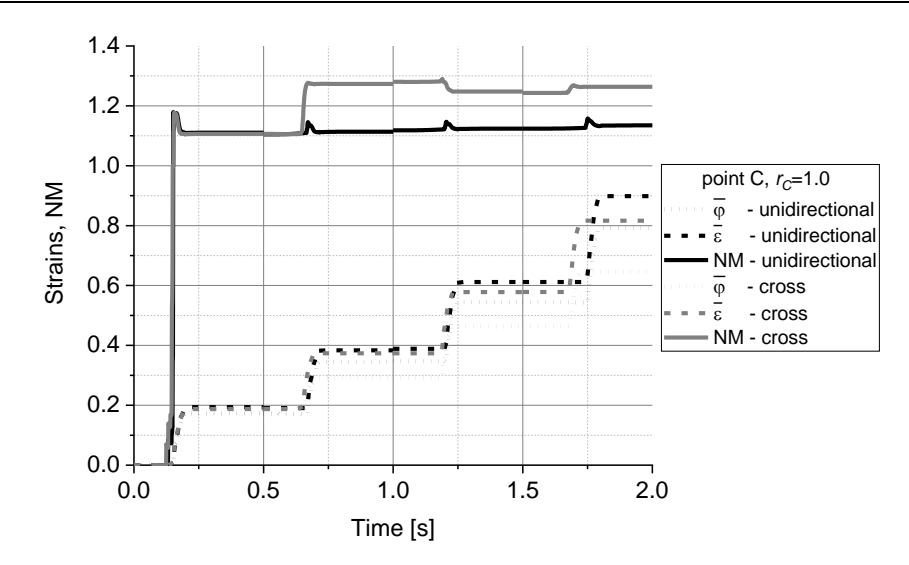
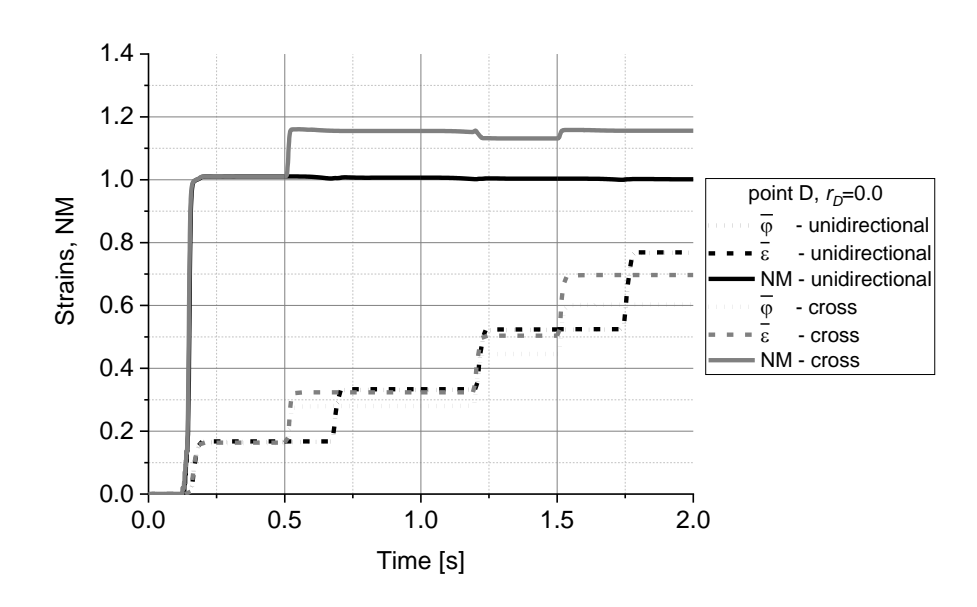


Figure 9

Logarithmic equivalent-, total equivalent strain and NM parameter in point C



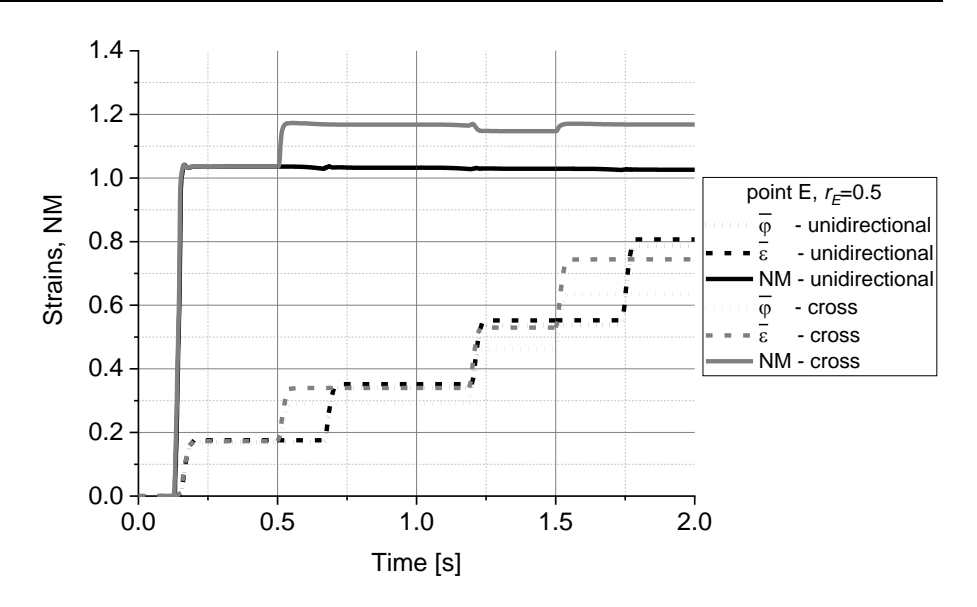


Figure 11
Logarithmic equivalent-, total equivalent strain and NM parameter in point E

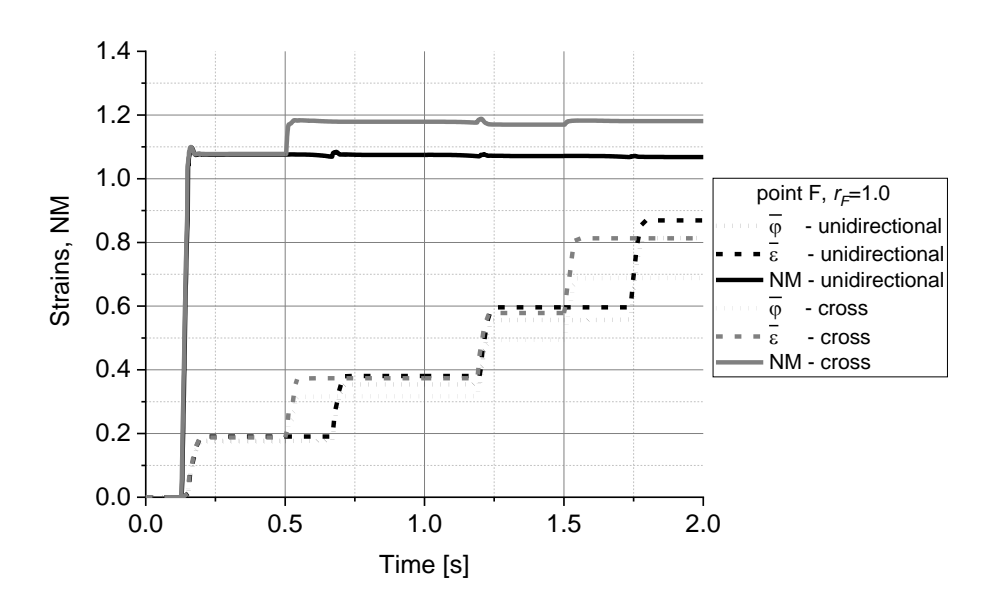


Figure 12
Logarithmic equivalent-, total equivalent strain and NM parameter in point F

A significant difference was observed in NM parameter of rolling methods. Cross rolling shows higher values of NM in each material points that confirms a higher degree of non-monotonicity of deformation. Figure 13 shows the calculated  $\cos \phi$  parameter of cross rolling in terms of transition between the passes. The parameter was investigated in different points of sheet. The horizontal dashed line designates the  $\cos \phi = 1.0$  which is a constant value and characterizes unidirectional rolling process in terms of monotonicity for each investigated material points.

Since both parameters show significant differences between the plastically formed sheets, it is highly recommended to study and measure the materials microstructure more deeply. In addition, it is expected a significant difference in crystallographic texture as well. On the other hand, the three-dimensional simulations provide input data of texture simulation with a relative high accuracy.

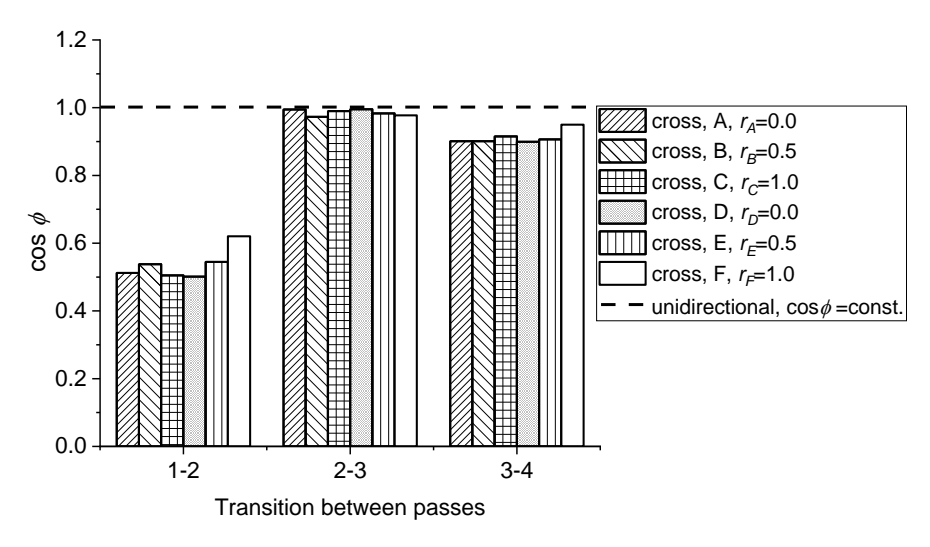


Figure 13
Comparison of  $\cos \phi$  parameter obtained two different rolling processes

## **CONCLUSION**

Three-dimensional finite element models were established to simulate the experimental rolling. Calculations were validated by the measured rolling force per pass. The difference between the calculated and measured data was minimized iterative while the friction factor was modified several times.

The effects of two different rolling methods on the non-monotonicity and mechanical quantities of material were studied by numerical calculations when the investigated sheets have the same initial geometry. We observed a relative high difference in the value of non-monotonicity of unidirectional- and cross rolling that indicates a significant microstructural changes of niobium sheet.

#### **ACKNOWLEDGEMENTS**

The research was carried out at the University of Miskolc, within the framework of the Thematic Excellence Program funded by the Ministry of Innovation and Technology of Hungary. (Grant Contract reg. nr.: NKFIH-846-8/2019)

The described study was carried out as part of the EFOP-3.6.1-16-2016-00011 Younger and Renewing University – Innovative Knowledge City – institutional development of the University of Miskolc aiming at intelligent specialisation project implemented in the framework of the Széchenyi 2020 program. The realization of this project is supported by the European Union, co-financed by the European Social Fund.

# REFERENCES

- [1] Rout, M., Pal, S. K., Singh, S. B. (2015). Cross Rolling: A Metal Forming Process. In: Davim, J. (ed.). *Modern Manufacturing Engineering. Materials Forming, Machining and Tribology*. Springer International Publishing, Switzerland.
- [2] Ilyushin, A. A. (1990). *Mehanika splosnoj sredi*. SSSR, Izdatelstvo Moskovskogo Universiteta, p. 196.
- [3] Krallics, G., Malgyn, D. (2005). Finite element simulation of equal channel angular pressing. In: Burhanettin, Altan (ed.). Severe Plastic Deformation: Towards Bulk Production of Nanostructured Materials. 612 p. New York, Nova Science Publishers Inc., p. 445.
- [4] Schmitt, J. H., Shen, E. L., Raphanel, J. L. (1994). A parameter for measuring the magni- tude of a change of strain path: Validation and comparison with experiments on low carbon steel. *International Journal of Plasticity*, 10, pp. 535–551.
- [5] Catorceno, Litzy Lina Choquechambi, de Abreu, Hamilton Ferreira Gomes, Padilha, Angelo Fernando (2018). Effects of cold and warm cross-rolling on microstructure and texture evolution of AZ31B magnesium alloy sheet. *Journal of Magnesium and Alloys*, 6, pp. 121–133.
- [6] Gurao, N. P., Sethuraman, S., Suwas, Satyam (2011). Effect of strain path change on the evolution of texture and microstructure during rolling of copper and nickel. *Materials Science and Engineering A*, 52, pp. 7739–7750.
- [7] Davenport, S. B., Higginson, R. L., Sellars, C. M., Withers, P. J., van Houtte, P., Brown, L. M., Prangnell, P. (1999). The Effect of Strain Path on Material Behaviour during Hot Rolling of FCC Metals. *Philosophical Transactions: Mathematical, Physical and Engineering Sciences*, Vol. 357, No. 1756, Deformation Processing of Metals, pp. 1645-1661.

- [8] Koohbor, Behrad, Serajzadeh, Siamak (2012). Influence of deformation path change on static strain aging of cold rolled steel strip. *International Journal of Advanced Manufacturing Technology*, 61, pp. 901–909.
- [9] Rout, Matruprasad, Pal, Surjya K., Singh, Shiv B. (2016). Finite element simulation of a cross rolling process. *Journal of Manufacturing Processes*, 24, pp. 283–292.